

## Dynamic behaviour of semi-rigid jointed cold-formed steel hollow frames

P. S. Joanna<sup>†</sup>

*Civil Engineering, Hindustan College of Engineering, Chennai, India*

G. M. Samuel Knight<sup>‡</sup>

*Civil Engineering, Anna University, Chennai, India*

A. Rajaraman<sup>‡†</sup>

*Department of Civil Engineering, I.I.T., Madras, India*

*(Received July 21, 2005, Accepted June 27, 2006)*

**Abstract.** This paper deals with the dynamic behaviour of cold-formed steel hollow frames with different connection stiffnesses. An analytical model of a semi-rigid frame was developed to study the influence of connection stiffnesses on the fundamental frequency and dynamic response of the frames. The flexibilities of the connections are modeled by rotational springs. Neglect of semi-rigidity leads to an artificial stiffening of frames resulting in shorter fundamental period, which in turn results in a significant error in the evaluation of dynamic loads. In the seismic design of structures, of all the principal modes, the fundamental mode of translational vibration is the most critical. Hence, experiments were conducted to study the influence of the connection stiffnesses on the fundamental mode of translational vibration of the steel hollow frames. From the experimental study it was found that the fundamental frequency of the frames lie in the semi-rigid region. From the theoretical investigation it was found that the flexibly connected frames subjected to lateral loads exhibit larger deflection as compared to rigidly connected frames.

**Keywords:** steel hollow frames; cold-formed; semi-rigid; dynamic response; fundamental frequency.

---

### 1. Introduction

The accuracy and reliability of an analysis depend heavily on the approximation of the model to the real structure. One of the major factors which contribute for an accurate model is the simulation of the connection behaviour under dynamic loads. The basic assumptions of conventional structural analysis in steel framework is that the joints are either perfectly rigid or ideally hinged. However, in actual structures, connections do not behave either in a perfectly rigid or perfectly hinged manner. In reality,

---

<sup>†</sup>Lecturer

<sup>‡</sup>Professor, Corresponding author, E-mail: [gmsk@annauniv.edu](mailto:gmsk@annauniv.edu)

<sup>‡†</sup>Visiting Professor

connections are semi-rigid and possess a certain degree of rotational restraint. Connection flexibility affects the fundamental frequency, force distribution and deformation in frames, and must be accounted in a dynamic structural analysis.

In spite of the extensive work on static analysis of semi-rigid steel frames, very few researchers have worked on the dynamic analysis of semi-rigid steel hollow frames. Chui and Chan (1996) have studied the transient response of moment-resistant steel frames with flexible joints. It was found that the displacement response of a structure with non-linear flexible connections will magnify under low harmonic vibrating loads, and will dampen under high harmonic vibrating loads. Lui and Lopes (1996) have analytically studied the dynamic response of semi-rigid frames using a computer model. The presence of connection flexibility tends to reduce frame stiffness, and hence increases the natural period of vibration of the frames. Dhillon and O'Malley (1999) analysed the semi-rigid jointed frames subjected to static loadings. Computer based analysis and design of semi-rigid steel frames subjected to static loadings were presented. Alfawakhiri and Bruneau (2000) have studied the interaction between superstructure and support flexibilities of simply supported bridges to ground motion. The bridges were modelled as beams with uniformly distributed mass and elasticity. It was illustrated through case studies that the total response could be evaluated with sufficient accuracy by taking into account only the contribution of the first mode, and neglecting the contribution of higher modes. Sekulovic *et al.* (2002) have studied the effects of flexibility in the nodal connections on the dynamic behaviour of plane steel frames. A flexible connection was idealized by a rotational spring. The dynamic stiffness matrix for the beam with flexible connection at its end was formulated. Examples were provided to illustrate the efficiency and accuracy of the method. It was concluded that the connection flexibility significantly alters both the vibration and the response of the frames. An increase in the connection flexibility reduces the frame stiffness, and thus the eigenfrequencies, particularly the lower values, which may have primary influence on the dynamic response of the structure. Ozturk and Secer (2005) have studied the dynamic response of semi-rigid steel frames. Connection flexibility was modelled by linear elastic rotational springs. It was concluded that the location of the linear elastic connection springs affects the behaviour and lateral rigidity of frames. Cabrero and Bayo (2005) proposed a method to optimise not only the size of the structural profiles, but also the joint design to make it fit to the optimal theoretical values. Pre-design methods for semi-rigid extended end-plate joints were also provided to check the feasibility and suitability of a connection design. Design examples were provided to demonstrate the application of the proposed semi-rigid design methods, and the results were compared to pinned and rigid connections. Joanna *et al.* (2005) studied the effect of connection flexibilities on the dynamic response of beams and frames. Connection flexibilities affect the force distribution and deformations in the beams and frames. Ungureanu and Dubina (2005) studied the seismic performance of cold-formed steel portal frames. It was concluded that the cold-formed steel structures could be designed to resist seismic actions using elastic design by taking the behaviour factor of 1.5 to 2. to evaluate the seismic design load.

The primary objective of the present study is to investigate the influence of connection flexibility on the fundamental frequency and dynamic response of semi-rigid jointed steel hollow frames. Semi-rigid connections are idealised by rotational springs. The element stiffness matrix is formulated including the flexibility of the connections and the structure stiffness matrix is obtained based on the conventional stiffness matrix analysis. Consistent mass matrix based on the deflected shape allowing for semi-rigidity of the connections is also derived. In the seismic design of structures, of all the principal modes, the fundamental mode of translational vibrations is the most critical one. Hence, only the translational degree of freedom is retained and all the other degrees of freedom of the frames are condensed out in the system stiffness matrix and the fundamental frequency in the translational mode has been found out.

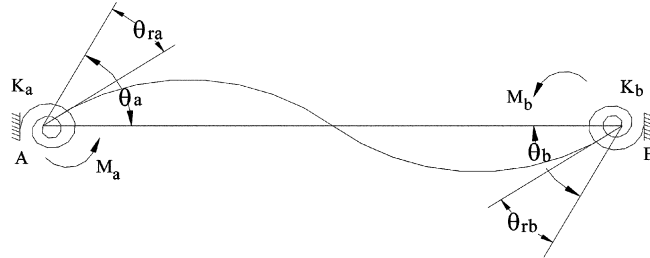


Fig. 1 Beam element of the frame with rotational springs

The theoretical results were compared with the experimental observations by testing six steel hollow frames. Modal analysis is then carried out to determine the lateral deflection and bending moment for the frame with the semi-rigid connections. Fundamental frequency versus spring stiffness behaviour, lateral deflection versus spring stiffness behaviour, column base moment versus spring stiffness behaviour, beam bending moment versus spring stiffness behaviour and the normalised behaviours of the frames with semi-rigid connection were presented.

## 2. Fundamental frequency for a frame with semi-rigid connection

### 2.1. Formulation of the static stiffness and consistent mass matrices with semi-rigid connection

The stiffness matrix for a semi-rigid frame element is derived by taking into account the rotational springs. For the beam element shown in Fig. 1 the relative rotations of springs  $\theta_{ra}$  and  $\theta_{rb}$  are related to spring stiffnesses  $K_a$  and  $K_b$  as

$$\theta_{ra} = M_a/K_a \text{ and } \theta_{rb} = M_b/K_b$$

The modified stiffness matrix is obtained by replacing the joint rotations  $\theta_a$  and  $\theta_b$  by  $(\theta_a - \theta_{ra})$  and  $(\theta_b - \theta_{rb})$  respectively as follows.

$$\begin{bmatrix} M_a \\ M_b \end{bmatrix} = \frac{1}{L} \begin{bmatrix} 4EI & 2EI \\ 2EI & 4EI \end{bmatrix} \begin{bmatrix} \theta_a - \theta_{ra} \\ \theta_b - \theta_{rb} \end{bmatrix} \quad (1)$$

$$M_a = \frac{4EI}{L} \left( \theta_a - \frac{M_a}{K_a} \right) + \frac{2EI}{L} \left( \theta_b - \frac{M_b}{K_b} \right) \quad (2)$$

$$M_b = \frac{4EI}{L} \left( \theta_b - \frac{M_b}{K_b} \right) + \frac{2EI}{L} \left( \theta_a - \frac{M_a}{K_a} \right) \quad (3)$$



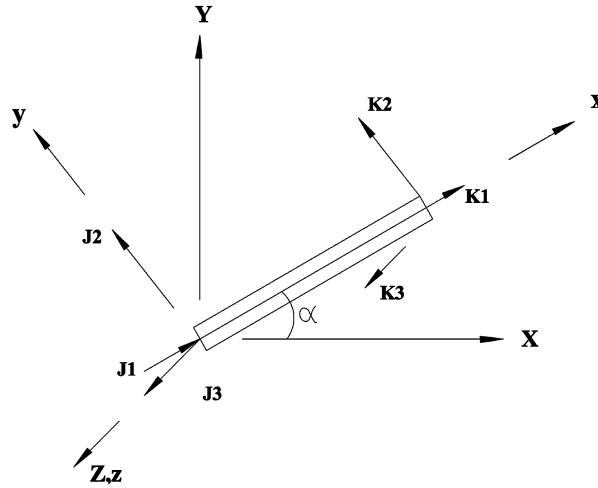


Fig. 2 Plane frame element in member (x, y, z) and structure (X, Y, Z) co-ordinates

### 2.2. Generalized stiffness matrix

The semi-rigid element stiffness matrix is in local or member co-ordinate system. It is necessary to transfer them to global or structure oriented co-ordinates before a complete structure stiffness matrix can be formed. The transformation is accomplished by the relation.

$$[K]_s = [T]_e^T [K]_e [T]_e$$

where  $[K]_s$  is the stiffness matrix for the member 'e' in structure co-ordinate system.

$[K]_e$  is the stiffness matrix for the member in the member co-ordinate system.

$[T]_e$  is the transformation matrix for the member of the form.

$$[T]_e = \begin{bmatrix} \cos \alpha & \sin \alpha & 0 & 0 & 0 & 0 \\ -\sin \alpha & \cos \alpha & 0 & 0 & 0 & 0 \\ 0 & 0 & 1 & 0 & 0 & 0 \\ 0 & 0 & 0 & \cos \alpha & \sin \alpha & 0 \\ 0 & 0 & 0 & -\sin \alpha & \cos \alpha & 0 \\ 0 & 0 & 0 & 0 & 0 & 1 \end{bmatrix} \quad (6)$$

where ' $\alpha$ ' is the angle between the structure and member co-ordinate systems.

### 2.3. Structure stiffness and static condensation

In order to find out the frequency in the translational mode of the frame, the rotational degrees of freedom and axial degrees of freedom are to be condensed out of the system stiffness relationship. The translational degree of freedom is separated from the other degrees of freedom and given as follows.

$$\begin{bmatrix} F(t) \\ 0 \end{bmatrix} = \begin{bmatrix} K_{tt} & K_{to} \\ K_{ot} & K_{oo} \end{bmatrix} \begin{bmatrix} U_t \\ U_o \end{bmatrix} \quad (7)$$

where  $U_t$  is a vector containing the translational degrees of freedom and  $U_o$  is a vector containing the other degrees of freedom.

From Eq. (7)  $F(t) = K_c U_t$ , where  $K_c = K_{tt} - K_{to}K_{oo}^{-1}K_{ot}$

The condensed mass matrix can also be found out in the same way as mentioned above. The frequency in the translational mode of vibration is found from the condensed stiffness and condensed mass matrix.

### 3. Experimental investigation

Experiments were conducted on six hollow steel frames of height 1 m and width 1.5 m with a side weld with transverse weld and with an end return weld, in order to study the effect of weld length on the fundamental frequency of the frame. The cross sections of the frames tested are given in Table 1.

Table 1 Cross sections of the frames tested

Frame No.	Hollow beam size mm × mm × mm	Hollow column size mm × mm × mm
1	80 × 40 × 2	100 × 50 × 2
2	80 × 40 × 2.6	100 × 50 × 2.6
3	40 × 40 × 2	50 × 50 × 2

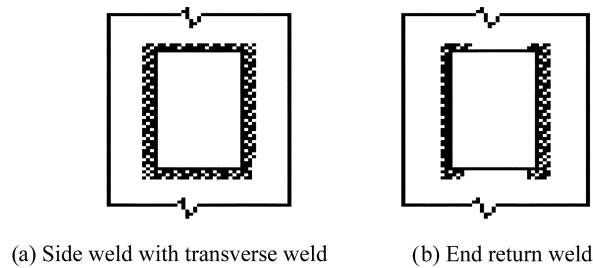
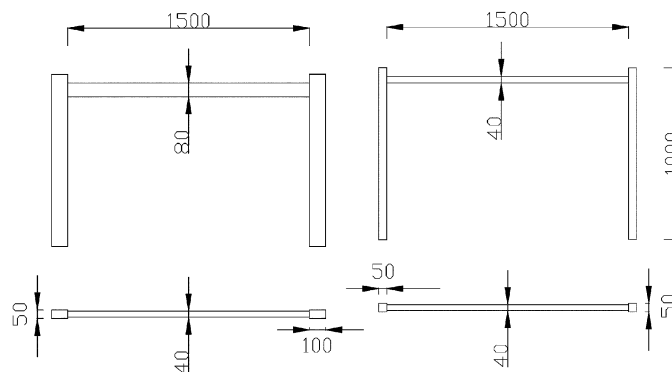


Fig. 3 Welded connections



All dimensions are in mm

Fig. 4 Test specimen details of the frame



(a) Measurement of the fundamental mode of translational vibration



(b) Test set-up for loading the frame



(c) The frame after failure

Fig. 5 Experimental set-up

The schematic views of the above welds are given in Fig. 3 and Fig. 4 shows the test specimen details.

The experiments were conducted in loading frame of capacity 40 T. The frames were given a small lateral displacement and the free lateral mode of vibration was picked up by the vibration sensor which was connected to the Cathode Ray Oscilloscope (CRO) as shown in Fig. 5(a). After the free vibration test, the frames were tested to failure to predict the failure mode of the frames. The frames were tested to failure by applying central concentrated static load on the beam as shown in Fig. 5(b) and no weld failure was noticed in any of the frames as shown in Fig. 5(c). Fig. 6 shows the frequency curves obtained from CRO for all the frames.

Translational frequencies of the frames are found by static condensation method for various connection stiffness of the frames and are shown in Figs. 7(a), 8(a) and 9(a). The frame is analysed from fixed end condition to simply supported condition allowing equal flexibility for all the connections. Figs. 7(b), 8(b) and 9(b) show the normalised fundamental frequency for the joint stiffness. The fundamental frequency is normalised by the fundamental frequency of the fully flexible joint.

It is seen that the fundamental frequency of the Frame 1 and Frame 2 is constant if the spring stiffness is less than 100 Nm/radian (i.e., fully flexible joints). Further increase of spring stiffness from 100 Nm/radian increases the fundamental frequency significantly and remains constant when the stiffness is

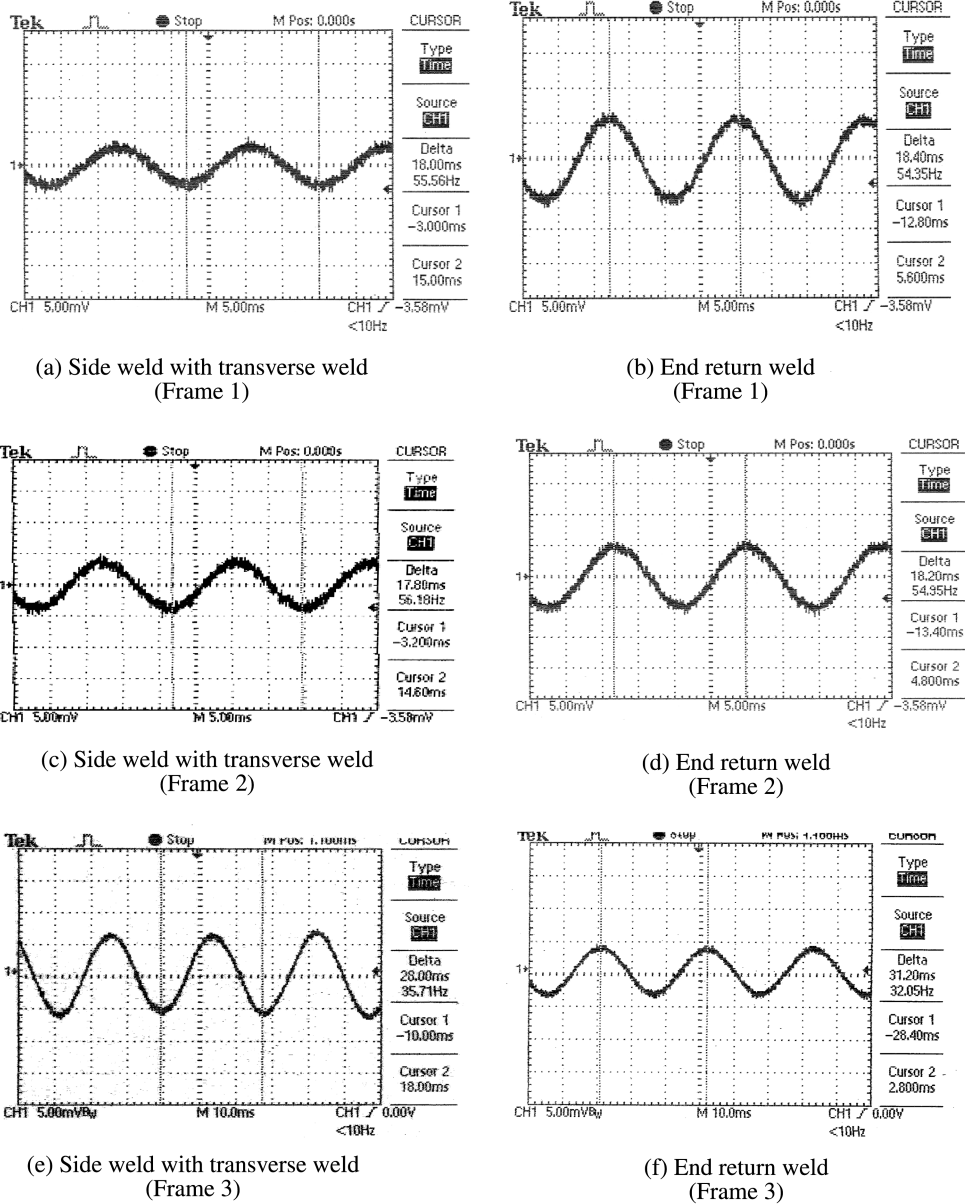


Fig 6. Frequency curves obtained through CRO

more than  $10^7$  Nm/radian (i.e., infinitely rigid joint). The spring stiffness is plotted in a log scale. It can be observed that the normalised fundamental frequency varies between 1 and 1.37 for the frames. The magnitude of the stiffness of the spring ' $K$ ' does not determine if a joint will behave in a rigid or flexible manner. Rather it is the ratio of the spring stiffness ' $K$ ' to the flexural stiffness of the beam member ' $EI_b/L$ ' that determines the type of behaviour that will be exhibited. This ratio is called joint stiffness. When the joint stiffness is less than 0.1, the frames behave as if it is hinged and if the joint stiffness is greater than 1000, the frames behave as if it is fixed. For joint stiffness values in between the

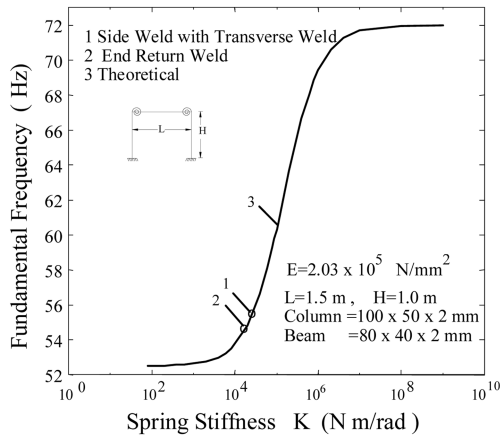


Fig. 7(a) Fundamental frequency vs. spring stiffness (Frame 1)

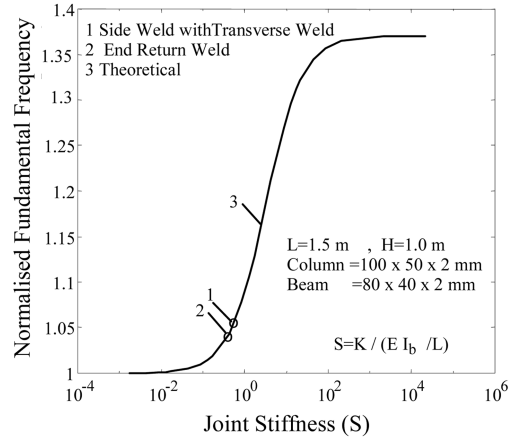


Fig. 7(b) Normalised fundamental frequency vs. joint stiffness (Frame 1)

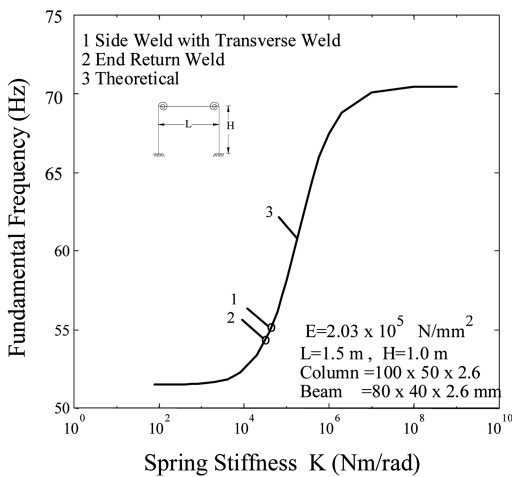


Fig. 8(a) Fundamental frequency vs. spring stiffness (Frame 2)

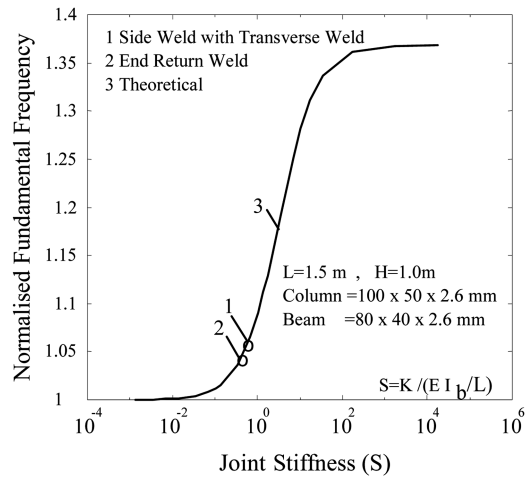


Fig. 8(b) Normalised fundamental frequency vs. joint stiffness (Frame 2)

above limits, the frames behave as a semi-rigid one. When the experimental values are fitted in to the theoretical frequency curve, they lie in the semi-rigid region.

It is seen that the fundamental frequency of the Frame 3 is constant if the spring stiffness is less than 100 Nm/radian (i.e., fully flexible joints). Further increase of spring stiffness from 100 Nm/radian increases the fundamental frequency significantly and remains constant when the stiffness is more than  $10^6$  Nm/radian (i.e., infinitely rigid joint). It can be observed that the normalised fundamental frequency varies between 1 and 1.32 for the Frame 3. When the joint stiffness is less than 0.1, the Frame 3 behaves as if it is hinged and if the joint stiffness is greater than 1000, the frame behaves as if it is fixed. For joint stiffness values in between the above limits, the frame behaves as a semi-rigid one. When the experimental values are fitted in to the theoretical frequency curve, they lie in the semi-rigid region. Thus the neglect of flexibility of the joint leads to artificial stiffening of the system resulting in higher fundamental frequency. Accurate determination of the fundamental frequency is essential in the

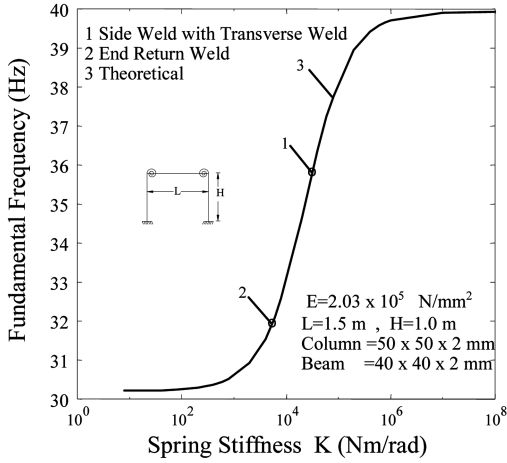


Fig. 9(a) Fundamental frequency vs. spring stiffness (Frame 3)

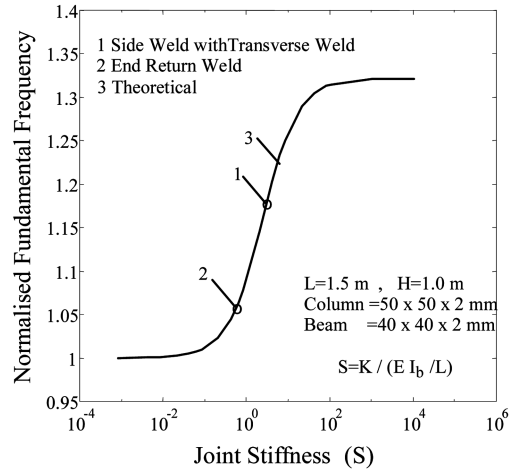


Fig. 9(b) Normalised fundamental frequency vs. joint stiffness (Frame 3)

evaluation of seismic loading, especially when design spectra exhibit short variation of response acceleration coefficient with fundamental frequency.

#### 4. Dynamic response of the frame with semi-rigid connection

##### 4.1. Lateral deflection of the frame

The frames with various connection stiffness are further studied on its dynamic response. A sudden concentrated lateral load of 4 kN is assumed to be applied to the Frame 1 and Frame 2 for a time period of ( $t/T = 0.5$ ), where  $T$  is the fundamental time period of the frame. The variation of the lateral deflection of

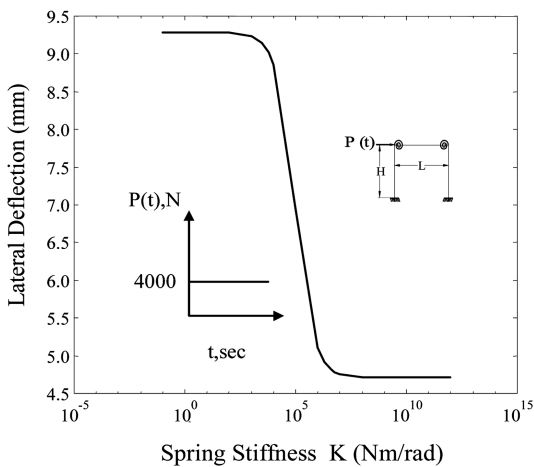


Fig. 10(a) Deflection vs. spring stiffness (Frame 1)

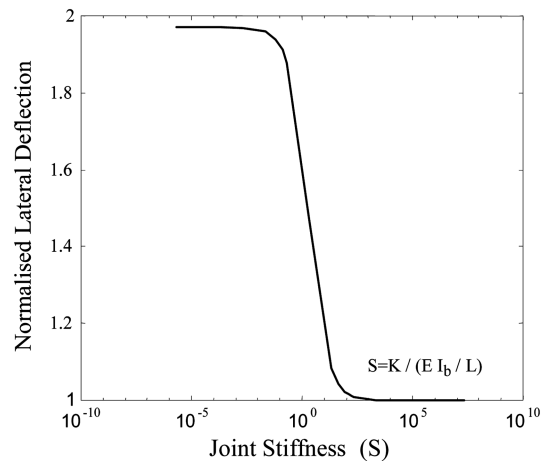


Fig. 10(b) Normalised deflection vs. joint stiffness (Frame 1)

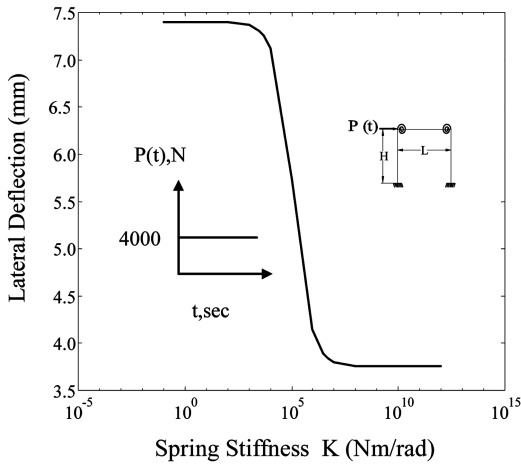


Fig. 11(a) Deflection vs. spring stiffness (Frame 2)

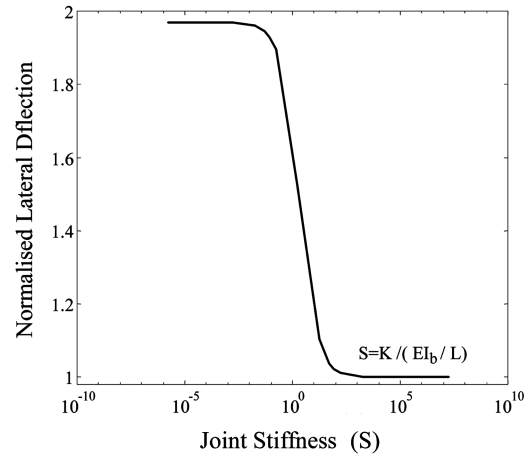


Fig. 11(b) Normalised deflection vs. joint stiffness (Frame 2)

the frames for the translational mode, depending on the magnitude of the spring stiffness is shown in Figs. 10(a) and 11(a). Figs. 10(b), 11(b) show the normalised deflection for the joint stiffness.

The sway deflection of both the frames increase with the connection flexibility. The lateral deflection is normalised by the lateral deflection of the fully rigid joint. The normalised lateral deflection varies between 1 and 1.95 for both the frames. Thus the deflection of the fully flexible frames increases by 50% than that of the rigid frames. From the normalised deflection curve it is seen, when the joint stiffness is less than 0.1, the frame behaves as if it is hinged and if the joint stiffness is greater than 1000, the frame behaves as if it is fixed. For joint stiffness values in between the above limits, the frame behaves as a semi-rigid one.

Fig. 12(a) shows the lateral deflection of the Frame 3 when a sudden concentrated lateral load of 2 kN is assumed to be applied for a time period of  $(t/T = 0.5)$  and Fig. 12(b) shows the normalised deflection for the joint stiffness.

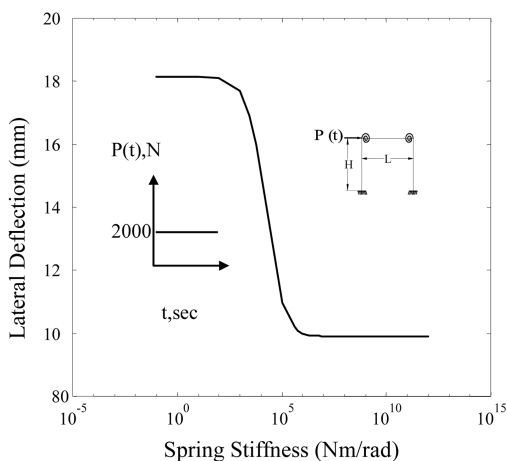


Fig. 12(a) Deflection vs. spring stiffness (Frame 3)

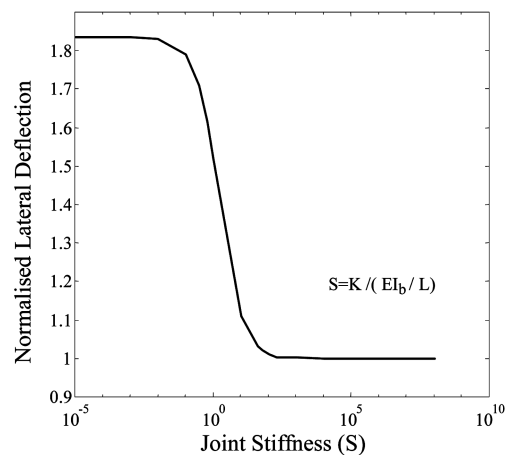


Fig. 12(b) Normalised deflection vs. joint stiffness (Frame 3)

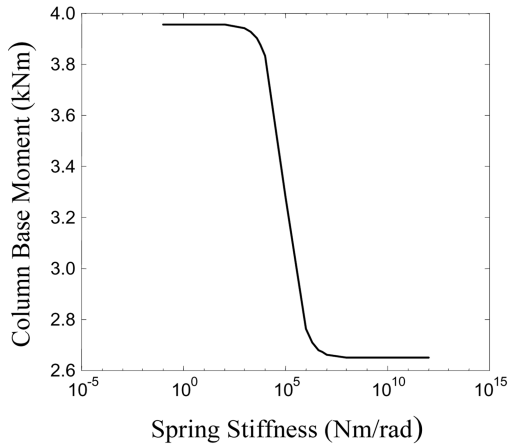


Fig. 13(a) Column base moment vs. spring stiffness (Frame 1)

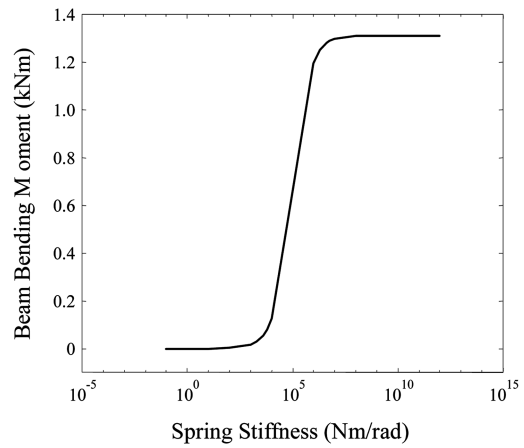


Fig. 13(b) Beam bending moment vs. spring stiffness (Frame 1)

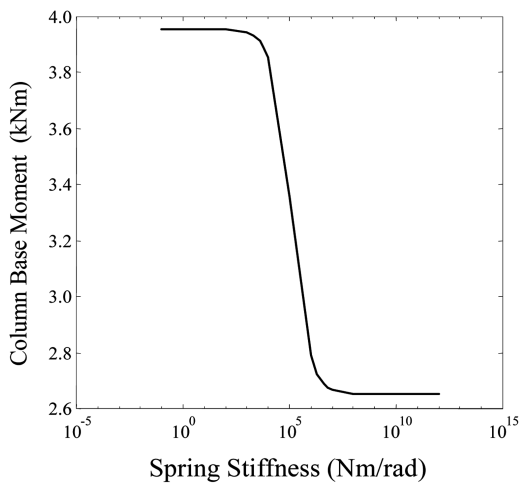


Fig. 14(a): Column base moment vs. spring stiffness (Frame 2)

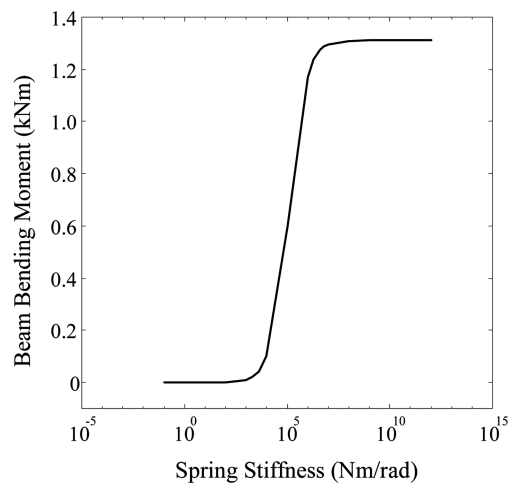


Fig. 14(b) Beam bending moment vs. spring stiffness (Frame 2)

The normalised lateral deflection varies between 1 and 1.84. Thus the deflection of the flexible frame increases by 50% than that of the rigid frame. Thus the serviceability sway criteria govern the design rather than the strength criteria since the stiffness of the semi-rigid jointed frame is smaller and it undergoes large lateral deflection.

#### 4.2. Beam and column moments

The variation of the bending moment at the bottom of the column depending on the magnitude of the spring stiffness is shown in Figs. 13(a), 14(a), 15(a) and Figs. 13(b), 14(b), 15(b) show the bending moment at the end of the beam for the various connection stiffness.

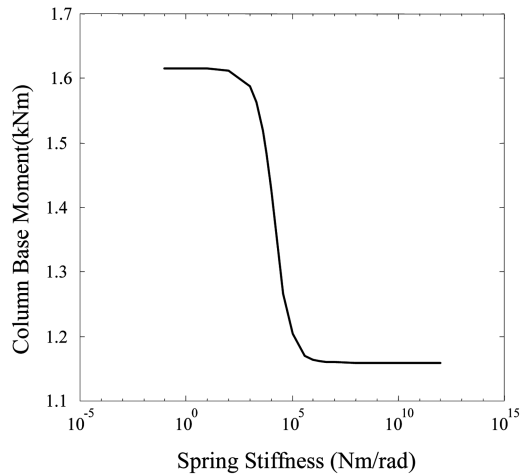


Fig. 15(a) Column base moment vs. spring stiffness (Frame 3)

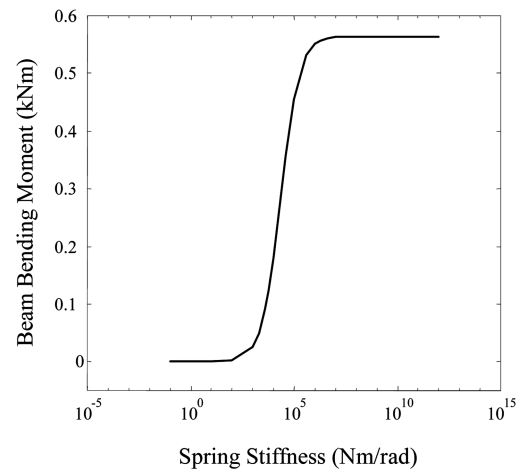


Fig. 15(b) Beam bending moment vs. spring stiffness (Frame 3)

The semi-rigidity in the connections causes a significant reduction in the beam bending moment. Thus the semi-rigidity in connections has advantageous effects on beam end bending moment. We see from this example that the semi-rigidity increases the column bending moments significantly. We also infer that if a real flexibly connected steel structure is idealized as having rigid joints, we may unconservatively estimate the column base moment.

## 5. Conclusions

The role of flexibility of joints in frames is studied both theoretically and experimentally and frames with rigid joint assumptions are re-analysed dynamically allowing for semi-rigid connections and the following conclusions are drawn.

- The connection stiffness affects the fundamental frequency of the frame significantly.
- The experimental study quantifies the errors made, when the assumptions of rigid connections are adopted in the dynamic analysis of frames.
- The fundamental frequency of the frames lies in the semi-rigid range for frames with side weld and transverse weld and also with end return weld.
- Neglect of semi-rigidity leads to an artificial stiffening of the frames, resulting in a shorter fundamental period, which leads to significant error in the evaluation of dynamic loads.
- When the joint stiffness is less than 0.1, the frames behave as if it is hinged and if the joint stiffness is greater than 1000, the frames behave as if it is fixed. For joint stiffness values in between the above limits, the connections may be beneficially modeled as semi-rigid.
- The presented curves for normalized fundamental periods facilitate quick assessment of the error involved and allow practicing engineers to identify the instances where such an error becomes significant.
- The flexibly connected frames subjected to lateral loads exhibit larger deflection than rigidly connected frames. Thus the serviceability sway criteria govern the design rather than the strength criteria since the semi-rigid jointed frames undergo large lateral deflection.

- The semi-rigidity in the frames is not only advantageous in the beam design of the frames but also govern the column design in the frames.

## References

- Alfawakhiri, F. and Bruneau, M. (2000), "Flexibility of superstructures and supports in the seismic analysis of simple bridges", *Earthq. Eng. Struct. Dyn.*, **29**, 711-729.
- Cabrero, J. M. and Bayo, E. (2005), "Development of practical design methods for steel structures with semi-rigid connections", *Eng. Struct.*, **27**, 1125-1137.
- Chui, P. P. T. and Chan, S. L. (1996), "Transient response of moment-resistant steel frames with flexible and hysteretic joints", *J. Construct. Steel Res.*, **39**, 221-243.
- Dhillon, Balaur S. and O'Malley, James W. (1999), "Interactive design of semi-rigid steel frames", *J. Struct. Eng.*, **125**, 556-564.
- Joanna, P. S., Samuel Knight, G. M. and Rajaraman, A. (2005), "Dynamic flexibility effects in structural response", *Proc. of 4th European Conf. on Steel and Composite Structures*, The Netherlands.
- Lui, E. M. and Lopes, A. (1996), "Dynamic analysis and response of semi-rigid frames", *J. Eng. Struct.*, **19**, 644-645.
- Ozturk, A. U. and Secer, M. (2005), "Dynamic analysis of semi-rigid frames", *Mathematical and Computational Applications*, **10**(1), 1-8.
- Sekulovic, M., Salatic, R. and Nefovska, M. (2002), "Dynamic analysis of steel frames with flexible connections", *Comput. Struct.*, **80**, 935-955.
- Ungureanu, V. and Dubina, D. (2005), "Post-critical behaviour and ductility of cold-formed steel sections", *Proc. of 4th European Conf. on Steel and Composite Structures*, The Netherlands.

## Appendix: Mass matrix for the frame element with semi-rigid connection

Fig. 16 shows the displacement curves corresponding to a unit displacement at each one of the nodal coordinates for a semi rigid beam segment of the frame having a uniform mass  $m(x) = m$  and a uniform stiffness  $EI(x) = EI$ , indicating the corresponding stiffness coefficients.

Fig. 16(a) shows the displacement curve for unit vertical displacement at the end 'A'. The bending moment is given by

$$EIu_2''(x) = K_{22}x - K_{32} \quad (8)$$

$$EIu_2'(x) = (K_{22}/2)x^2 - K_{32}x + C_{21} \quad (9)$$

$$EIu_2(x) = (K_{22}/6)x^3 - (K_{32}/2)x^2 + C_{21}x + C_{22} \quad (10)$$

The constants of integration  $C_{21}$  and  $C_{22}$  are evaluated using the boundary conditions of the beam segment of the frame with semi rigid connection when unit vertical displacement is given at 'A'.

Fig. 16(b) shows the displacement curve for unit rotation at the end 'A'. The bending moment is given by

$$EIu_3''(x) = K_{23}x - K_{33} \quad (11)$$

$$EIu_3'(x) = (K_{23}/2)x^2 - K_{33}x + C_{31} \quad (12)$$

$$EIu_3(x) = (K_{23}/6)x^3 - (K_{33}/2)x^2 + C_{31}x + C_{32} \quad (13)$$

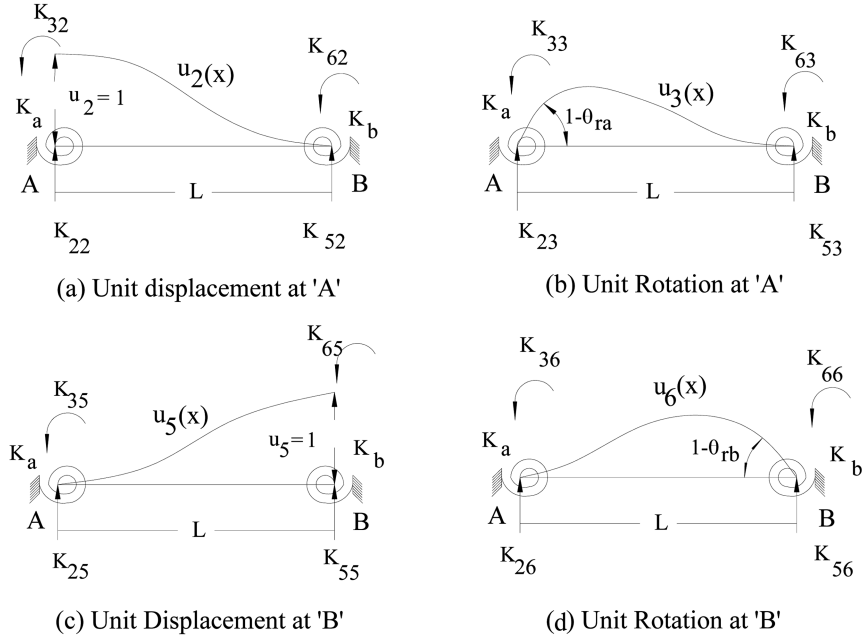


Fig. 16 Deflection curves due to unit displacement at one of the nodal co-ordinates

The constants of integration  $C_{31}$  and  $C_{32}$  are evaluated using the boundary conditions of the beam segment of the frame with semi-rigid connection when unit rotation is given at 'A'.

Fig. 16(c) shows the displacement curve for unit vertical displacement at the end 'B'. The bending moment is given by

$$Elu_5''(x) = K_{25}x - K_{35} \tag{14}$$

$$Elu_5'(x) = (K_{25}/2)x^2 - K_{35}x + C_{51} \tag{15}$$

$$Elu_5(x) = (K_{25}/6)x^3 - (K_{35}/2)x^2 + C_{51}x + C_{52} \tag{16}$$

The constants of integration  $C_{51}$  and  $C_{52}$  are evaluated using the boundary conditions of the beam segment of the frame with semi rigid connection when unit vertical displacement is given at 'B'.

Fig. 16(d) shows the displacement curve for unit rotation at the end 'B'. The bending moment is given by

$$Elu_6''(x) = K_{26}x - K_{36} \tag{17}$$

$$Elu_6'(x) = (K_{26}/2)x^2 - K_{36}x + C_{61} \tag{18}$$

$$Elu_6(x) = (K_{26}/6)x^3 - (K_{36}/2)x^2 + C_{61}x + C_{62} \tag{19}$$

The constants of integration  $C_{61}$  and  $C_{62}$  are evaluated using the boundary conditions of the beam with semi-rigid connection when unit rotation is given at 'B'.

The deflected curves  $u_1(x)$  and  $u_4(x)$  for axial effects of the beam element of the frame can be found by applying unit axial displacement at the end 'A' and 'B' respectively. The equations of the deflected curves can be used directly in the formulation of the mass matrix as follows.

$$[M_{ij}] = \int_0^L m u_i(x) u_j(x) dx \quad (20)$$

in which 'm' is the mass per unit length of the element. The mass matrix [M] for prismatic members can be, therefore, evaluated directly as below

$$m_{11} = \int_0^L m u_1(x) u_1(x) dx = \int_0^L m \left(1 - \frac{x}{L}\right) \left(1 - \frac{x}{L}\right) dx \quad (21)$$

$$m_{22} = \int_0^L m u_2(x) u_2(x) dx \quad (22)$$

$$= \int_0^L \frac{m}{(EI)^2} [(K_{22}/6)x^3 - (K_{32}/2)x^2 + C_{21}x + C_{22}][(K_{22}/6)x^3 - (K_{32}/2)x^2 + C_{21}x + C_{22}] dx$$

$$m_{32} = \int_0^L m u_3(x) u_2(x) dx \quad (23)$$

$$= \int_0^L \frac{m}{(EI)^2} [(K_{23}/6)x^3 - (K_{33}/2)x^2 + C_{31}x + C_{32}][(K_{22}/6)x^3 - (K_{32}/2)x^2 + C_{21}x + C_{22}] dx$$

$$m_{33} = \int_0^L m u_3(x) u_3(x) dx \quad (24)$$

$$= \int_0^L \frac{m}{(EI)^2} [(K_{23}/6)x^3 - (K_{33}/2)x^2 + C_{31}x + C_{32}][(K_{23}/6)x^3 - (K_{33}/2)x^2 + C_{31}x + C_{32}] dx$$

$$m_{41} = \int_0^L m u_4(x) u_1(x) dx = \int_0^L m \left(1 - \frac{x}{L}\right) \left(\frac{x}{L}\right) dx \quad (25)$$

$$m_{44} = \int_0^L m u_4(x) u_4(x) dx = \int_0^L m \left(\frac{x}{L}\right) \left(\frac{x}{L}\right) dx \quad (26)$$

$$m_{52} = \int_0^L m u_5(x) u_2(x) dx \quad (27)$$

$$= \int_0^L \frac{m}{(EI)^2} [(K_{25}/6)x^3 - (K_{35}/2)x^2 + C_{51}x + C_{52}][(K_{22}/6)x^3 - (K_{32}/2)x^2 + C_{21}x + C_{22}] dx$$

$$m_{53} = \int_0^L m u_5(x) u_3(x) dx \quad (28)$$

$$= \int_0^L \frac{m}{(EI)^2} [(K_{25}/6)x^3 - (K_{35}/2)x^2 + C_{51}x + C_{52}][(K_{23}/6)x^3 - (K_{33}/2)x^2 + C_{31}x + C_{32}] dx$$

$$m_{55} = \int_0^L m u_5(x) u_5(x) dx \quad (29)$$

$$= \int_0^L \frac{m}{(EI)^2} [(K_{25}/6)x^3 - (K_{35}/2)x^2 + C_{51}x + C_{52}] [(K_{25}/6)x^3 - (K_{35}/2)x^2 + C_{51}x + C_{52}] dx$$

$$m_{62} = \int_0^L m u_6(x) u_2(x) dx \quad (30)$$

$$= \int_0^L \frac{m}{(EI)^2} [(K_{26}/6)x^3 - (K_{36}/2)x^2 + C_{61}x + C_{62}] [(K_{22}/6)x^3 - (K_{32}/2)x^2 + C_{21}x + C_{22}] dx$$

$$m_{63} = \int_0^L m u_6(x) u_3(x) dx \quad (31)$$

$$= \int_0^L \frac{m}{(EI)^2} [(K_{26}/6)x^3 - (K_{36}/2)x^2 + C_{61}x + C_{62}] [(K_{23}/6)x^3 - (K_{33}/2)x^2 + C_{31}x + C_{32}] dx$$

$$m_{65} = \int_0^L m u_6(x) u_5(x) dx \quad (32)$$

$$= \int_0^L \frac{m}{(EI)^2} [(K_{26}/6)x^3 - (K_{36}/2)x^2 + C_{61}x + C_{62}] [(K_{25}/6)x^3 - (K_{35}/2)x^2 + C_{51}x + C_{52}] dx$$

$$m_{66} = \int_0^L m u_6(x) u_6(x) dx \quad (33)$$

$$= \int_0^L \frac{m}{(EI)^2} [(K_{26}/6)x^3 - (K_{36}/2)x^2 + C_{61}x + C_{62}] [(K_{26}/6)x^3 - (K_{36}/2)x^2 + C_{61}x + C_{62}] dx$$

$$m_{21} = m_{31} = m_{41} = m_{42} = m_{43} = m_{51} = m_{54} = m_{61} = m_{64} = 0 \quad (34)$$